Journal of Research in Pharmacy

Research Article

www.jrespharm.com

Lisinopril dihydrate loaded nano-spanlastic bio-adhesive gel for intranasal delivery: 2^3 factorial optimization, fabrication and ex-vivo studies for enhanced mucosal permeation

Suresh PRIYANKA[1], **Radhakrishnan NITHYA**[1*]

[1] Department of Pharmaceutics, Faculty of Pharmacy, PSG College of Pharmacy, Coimbatore, India.

* Corresponding Author. E-mail: 82nithikrish@gmail.com (R.N); Tel. +91-978-888 70 41.

Received: 5 January 2022 / Revised: 13 April 2022 / Accepted: 13 April 2022

ABSTRACT: Lisinopril dihydrate (LP) is an FDA approved drug used in the treatment of hypertension. When administered orally it is slowly and incompletely absorbed with a bioavailability of 25–30% only. The aim of the present study is to increase the bioavailability of LP by formulating into nano-spanlastic bio-adhesive gel for intranasal delivery. LP loaded nano-spanlastics (LPSp) were prepared by ethanol injection method according to 2^3 factorial designs using Design Expert® software, to explore the impact of different independent variables on Particle Size (PS) and Entrapment efficiency (EE%). The optimized LPSp was evaluated for PS, surface morphology, polydispersity index (PDI), zeta potential, EE% and in-vitro drug release. Further, the optimized LPSp was loaded into Carbopol gel base (1%) and evaluated for pH, percentage drug content, texture properties and rheology. The permeation and histopathological studies were carried out using goat nasal mucosa. The optimized LPSp possessed spherical shape with PS and EE% of 320±4.5 nm and 72±2.5% respectively. Drug release studies revealed that the drug enclosed in spanlastic dispersion showed higher drug release compared to niosome dispersion. The LPSp gels exhibited satisfactory results for pH, drug content, texture properties and rheology. The ex-vivo results showed that the permeation rate of LP loaded nano-spanlastic bio-adhesive gel (LPSpG) increased when compared to that of LP loaded niosome gel (LPNiG). The results infer that encapsulating LP into vesicular carriers and formulating into a bio-adhesive gel augments its permeation and increases the residence time in nasal mucosa and therefore enhances its bioavailability.

KEYWORDS: Lisinopril dihydrate; spanlastic; edge activator; permeation; intranasal route; bio-adhesive gel.

1. INTRODUCTION

Innovative formulation designs that promote efficient drug delivery have resulted in successful treatment effects. This has allowed researchers to overcome several significant obstacles posed by the nature of the pathological condition, the body's physiology, or the drug's inherent qualities. Several methods are being adopted to enhance the bioavailability by encapsulating the drug in an appropriate carrier system. Nano vesicles are colloidal drug carriers which are known to possess certain advantages such as prolonged subsistence of the therapeutic agent in the systemic circulation, minimized toxicity due to selective uptake, improved bioavailability and encapsulation of both hydrophilic and lipophilic drug [1].

Vesicular carriers are novel drug delivery devices designed by formulation scientists to mimic nature's cellular material transport and survival systems [2]. They are nano-particulate systems formed by both lipophilic and hydrophilic polymers assembled in concentric lipid bilayers. It is built up with phospholipids or surfactants arranged in a circular structure that resembles micelle formation. It is a highly ordered assembly of one or more concentric lipid bilayers formed when amphiphilic building blocks are confronted with water [3]. The lipid bilayer entraps the lipophilic drugs whereas the aqueous core entraps the hydrophilic drugs. Vesicular carriers are associated to naturally prevailing vesicles in the human body and their innate physicochemical properties facilitates in an energy-controlled process, to self-assemble thereby forming vesicles. They are promising substitutes for the administration of drugs with challenging properties such as decreased solubility, poor absorption and permeation and reduced stability. This drug delivery system holds promise in view of its capacity to encapsulate both hydrophilic and lipophilic drug molecules and create stable complexes with them. Among the existing vesicular carrier systems such as liposomes, niosomes, transferosomes, ethosomes, pharmacosomes, etc. spanlastic systems are being explored as potential carriers for intranasal, topical and ocular delivery of certain drugs.

How to cite this article: Priyanka S, Nithya R. Lisinopril dihydrate loaded nano-spanlastic bio-adhesive gel for intranasal delivery: 23 factorial optimization, fabrication and ex-vivo studies for enhanced mucosal permeation. J Res Pharm. 2022; 26(4): 884-899.

http://dx.doi.org/10.29228/jrp.187

ISSN: 2630-6344

Spanlastic systems (span+elastic) are surface modified niosomes made up of non-ionic surfactants along with a membrane modifier called as edge activator [4]. An edge activator is a bilayer softening component which increases the elasticity of the vesicular membrane and therefore results in augmented permeation of the drug into the deeper layers of the skin by aiding in squeezing of the vesicular carriers containing the drug through the intracellular spaces of the skin [5].

Lisinopril dihydrate (LP) is an FDA approved drug used to treat hypertension. It competitively inhibits Angiotensin Converting Enzyme (ACE) and prevents Angiotensin I to Angiotensin II (an effective vasoconstrictor) conversion [6]. After oral intake the bioavailability of LP is only 25-30%. LP belongs to BCS class III (high solubility and poor permeability) [7]. Since it has high solubility, the poor bioavailability of the drug might be due to the following factors, (i) high hepatic first pass metabolism and (ii) decreased permeability of the drug through the intestinal mucosa. To overcome the above limitations and ameliorate the bioavailability of LP, an alternative route of delivery can be propounded.

In this study, to surmount the drawbacks of LP, an alternative route of delivery was chosen. Intranasal route of delivery, a more effective route that delivers the drug through the nose which ensures a rapid absorption of most drugs and can generate high systemic blood levels is preferred [8]. The barriers in this route of delivery such as drug permeability and residence time are overcome by encapsulating the drug into spanlastic vesicle and formulating it into a bio-adhesive gel. Encapsulating the drug into a vesicular carrier augments the permeation of LP in nasal mucosa and therefore enhances its bioavailability.

2. RESULTS AND DISCUSSION

2.1 Fourier Transform-Infra Red Spectroscopy (FT-IR) studies

The FTIR spectra of LP, Span 60, Tween 80, Physical mixture and LPSp were recorded. LP exhibited a set of bands between 3300 to 3200 cm^{-1} and 3000 to 2700 cm^{-1}. This might be due to N–H stretching of primary amines and O-H stretching of carboxylic acid respectively. A peak at 1600 cm^{-1} represents C-H bending of aromatic compound [9]. Span 60 showed a characteristic peak at 3231 cm^{-1} which is due to aliphatic O-H stretching, set of bands from 3000 cm^{-1} to 2840 cm^{-1} due to C–H stretch (alkane group) and peak from 1750-1735 cm^{-1} represents C=O stretch of ester [10]. Tween 80 exhibited peaks between 3000-2800 cm^{-1} which might be due to C-H stretching of alkane group. The peak at 1780 cm^{-1} is due to C=O of ester [11]. There was no disappearance of typical peaks in the FTIR spectra of the physical mixture and LPSp. This suggests that there were no intermolecular interactions between LP, Span 60, and Tween 80.

2.2 Formulation of LPSp dispersion

LPSp dispersions were successfully prepared with Span 60 and EA's (Tween 60 and Tween 80). Their physical appearance and stability were evaluated (Table 1). Milky white dispersions were formed. Formulations F1, F2, F6 and F7 were highly viscous due to higher concentration of Span 60. As the concentration of Span 60 is increased viscosity of formulation also increased. This is due to the high transition temperature (T_c=53°C) at which they act as gelators by themselves [12]. Span 60 was selected for the formulation since it imparts more sustainability due to presence of saturated alkyl chains [13]. The lipophilic nature of saturated alkyl chains permits formation of unilamellar/multilamellar matrix vesicles. Other forms of Span (Span 80 and Span 40) were not selected since they showed high degree of disruption, aggregation and instability [14]. Similarly, polysorbates (Tweens) were chosen for the formulation as they have been mentioned to be popularly used in the formulation of flexible vesicular carriers due to higher HLB value which increases the deformability of the vesicles by changing the packing characteristics [2,15].

From the Table 2, it is observed that LPSp dispersions containing Tween 80 as edge activator showed minimum PS of 92.67 nm and maximum EE% of 87.80 %. Therefore, the selection of suitable level of different variables was done with Tween 80 as EA, and by using different concentrations of Span 60 and EA, at two different speeds of rotation (300 and 800 rpm). A total of eight LPSp formulations were prepared and evaluated to obtain the optimized formulation.

Table 1. Physical appearance of LPSp dispersions

Formulation code	Physical Appearance
F1	Milky white viscous liquid
F2	Milky white viscous liquid
F3	Milky white semi viscous liquid
F4	Milky white liquid
F5	Milky white liquid
F6	Milky white viscous liquid
F7	Milky white viscous liquid
F8	Milky white semi viscous liquid
F9	Milky white liquid
F10	Milky white liquid

Table 2. Pre-screening study for the formulation of LPSp dispersions using tween 80 and tween 60 as EA

Formulation code	Ratio of Span 60 to Tween 80/Cholestrol	Ratio of Span 60 to Tween 60	PS (nm)	EE (%)
F1	90:10	-	657.40±2.95	76.80±2.80
F2	80:20	-	351.10±7.19	87.80±3.70
F3	70:30	-	155.90±5.82	72.16±4.39
F4	60:40	-	244.50±5.60	85.52±3.05
F5	50:50	-	92.67±3.25	62.92±5.90
F6	-	90:10	514.10±6.14	77.32±5.03
F7	-	80:20	372.60±6.90	55.76±6.24
F8	-	70:30	337.85±8.45	74.16±4.65
F9	-	60:40	203.21±7.32	60.00±3.97
F10	-	50:50	178.30±8.90	78.08±3.46

***n=3**

2.3 Analysis of 2^3 factorial design of LPSp dispersion

Table 3 depicts the actual design of 2^3 factorial designs which were typically used for understanding whether the factors are important in processing the formulation. This can be considered as a screening process to find out few important factors from many possibilities, or to indicate how known factors interact and individually effect the process. It provides the optimized formula by analyzing the effect of factors such as concentration of Span 60 (%), concentration of EA (%) and Speed of rotation (rpm) on the responses i.e., PS (nm) and EE (%) of the formulation. The relationship between factors and responses were elucidated and graphically illustrated by contour plot. The design was analyzed by identifying significant factor effects and by separating it from insignificant effects and pure error.

The statistics of the present model was depicted in table 4, the adequate precision values for PS and EE% was found to be more than 4 i.e., 12.277 and 13.697 respectively, indicating adequate model discrimination. The proposed model was able to meet the requirements for optimal precision values and optimal response values for operating the design space. The predicted R^2 value was computed to estimate response value's predictability. The adjusted R^2 is a reformed category of R^2 that accounts for independent variables that are not significant in a regression model. The predicted R^2 was in reasonable agreement with

the Adjusted R^2 i.e., the difference is less than 0.2. These results showed that the acquired data are more statistically valid and form an excellent fit to the obtained data [16].

Table 3. The 2^3 factorial design and the composition of LPSp containing tween 80 as EA

Run	Variables				
	Factors			Responses	
	X1	X2	X3	YI	Y2
1	50	50	800	93	90
2	90	10	800	458	86
3	90	50	800	658	95
4	50	10	800	312	84
5	50	10	300	279	75
6	90	50	300	402	87
7	50	50	300	187	84
8	90	10	300	377	90

Factors	Levels	
	Low	High
(X1): Concentration of Span 60 (%)	50	90
(X2): Concentration of EA (%)	10	50
(X3): Speed of rotation (rpm)	300	800

Table 4. Model statistics data of 2^3 factorial design of LPSp dispersion.

Responses	R^2	Adjusted R^2	Predicted R^2	Adequate precision
PS (Y1)	0.8708	0.8385	0.7703	12.277
EE%(Y2)	0.8774	0.8328	0.7406	13.697

The reliability and goodness of fit of the present model were also investigated from the diagnostic plots of PS and EE% of the LPSp dispersions represented in Figure 1. Figures 1a and 1c investigated the normal probability plots of residuals as a linear pattern with a normal distribution of the residuals. Therefore, the data required no alteration. Figures 1b and 1d analyzed a good resemblance between the predicted and the observed values of Y1and Y2 of LPSp dispersions in the present model.

ANOVA analysis (Table 5) was performed to comprehend the significance of various independent variables. The p-value that is lower than the threshold level (0.05), demonstrates the model terms significance.

Table 5. ANOVA results for the 2^3 factorial designs of LPSp dispersions.

Factors	Source	Sum of Squares	Degrees of freedom	Mean Square	F-value	p-Value	
	Model	4.424+05	3	1.475+05	26.96	< 0.0001	
PS	X1	3.318+05	1	3.318+05	60.66	< 0.0001	Significant
(Y1)	X2	441.00	1	441.00	0.0806	0.7813	
	X3	4.424+05	3	1.475+05	26.96	< 0.0001	
	Model	635.00	4	158.75	19.68	< 0.0001	
EE%	X1	210.25	1	210.25	26.06	0.0003	Significant
(Y2)	X2	2.25	1	2.25	0.2789	0.6079	
	X3	182.25	1	182.25	22.59	0.0006	

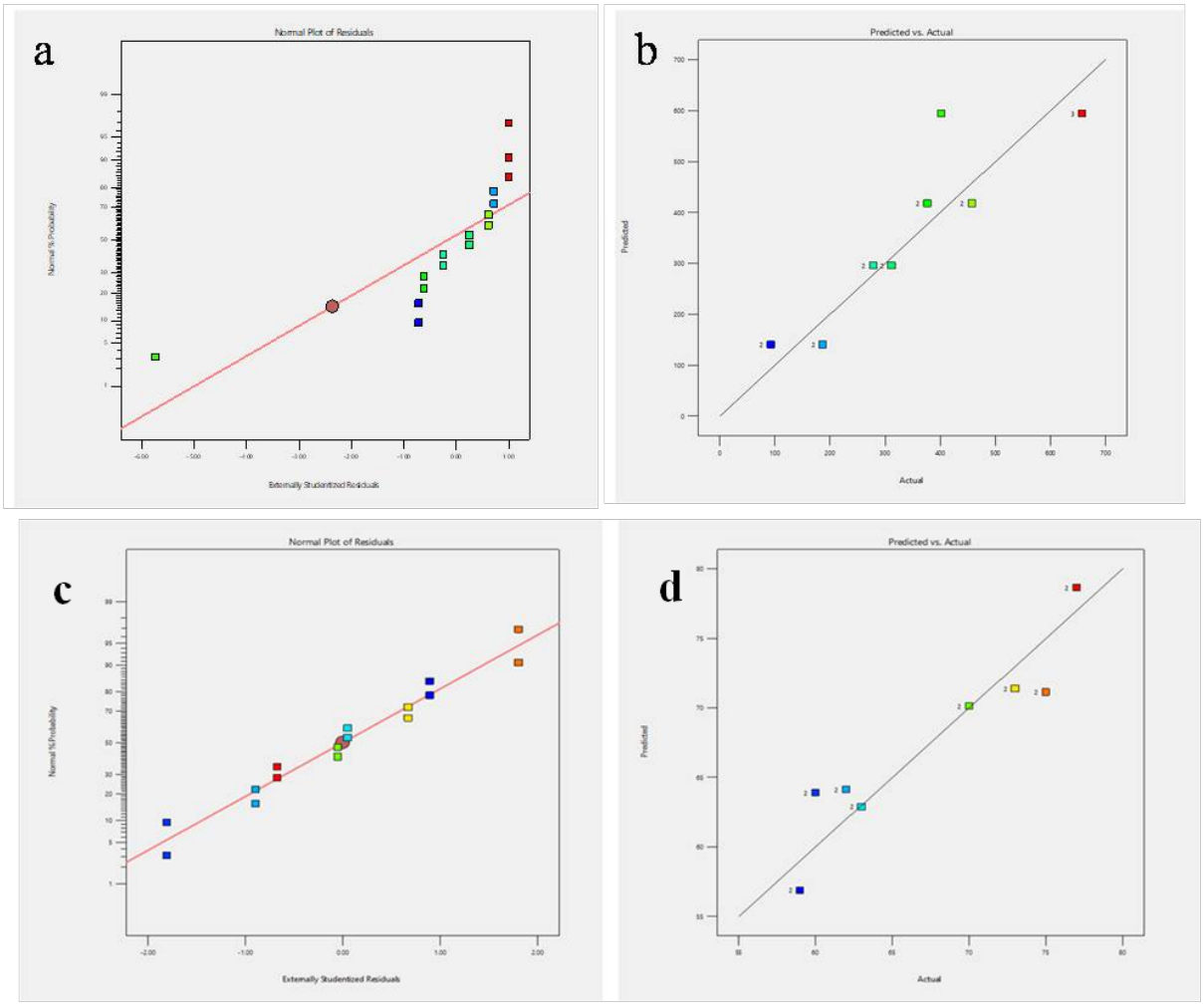

Figure 1. The diagnostic plots for PS and EE% of LPSp (a) plot of normal % probability versus the externally studentized residuals for PS, (b) plot of the predicted versus the actual values of PS and (c) plot of normal % probability versus the externally studentized residuals for EE%, and (b) plot of the predicted versus the actual values of EE%

2.4 Effect of factors on PS of LPSp dispersions

Table 3 shows that PS of LPSp dispersions ranged between 93 nm to 658 nm. The influence of the three different factors (X1, X2 and X3) on the PS of LPSp dispersions was studied (Figure 2). The results of ANOVA (Table 5) exhibited that the concentration of span 60 (X1), significantly affected the PS of LPSp dispersions. The PS of the formulated LPSp dispersion increased significantly ($p < 0.01$) upon increasing the concentration of span 60 (Figure 2a). This may be attributed to the inclusion of more alkyl chains of Span 60 into hydrophobic sphere of the vesicles following reduction in the interaction between polar heads of EA [14]. It was seen that the concentration of EA had no effect on the PS of the LPSp dispersion (Figure 2b). The PS of the LPSp dispersion was significantly ($p<0.01$) affected by the speed of rotation. On increasing the speed of rotation, the PS of the formulated nano spanlastics also increased (Figure 2c). This was due to the formation of highly viscous dispersion that forms aggregates of vesicles [17].

2.5 Effect of factors on percentage EE% of LPSp dispersions.

Table 3 displays that the percentage EE% of LPSp dispersions ranged from 84% to 95%. The influence of the three different factors (X1, X2 and X3) on the EE% of LPSp dispersions was investigated (Figure 2). The ANOVA results (Table 5) indicates that the concentration of span (X1), significantly affected the EE% of LPSp dispersions. The EE% of the formulated LPSp dispersions increased significantly ($p< 0.01$) on simultaneous increase in the concentration of span 60 (Figure 2d). This may be due to the higher phase transition temperature (T_c = 53 °C) and presence of saturated alkyl chain of Span 60, that results in reducing the leakage of drug from Span 60-based vesicles [18]. It was seen that the concentration of EA showed no effect on the EE% of the LPSp vesicles (Figure 2e). The EE% of the LPSp vesicle was significantly ($p<0.01$) affected by the speed of rotation. The EE % of the formulated nano-spanlastics increased, by increasing the speed of rotation (Figure 2f). This might be due to increased size of the vesicle due to formation of highly viscous dispersion.

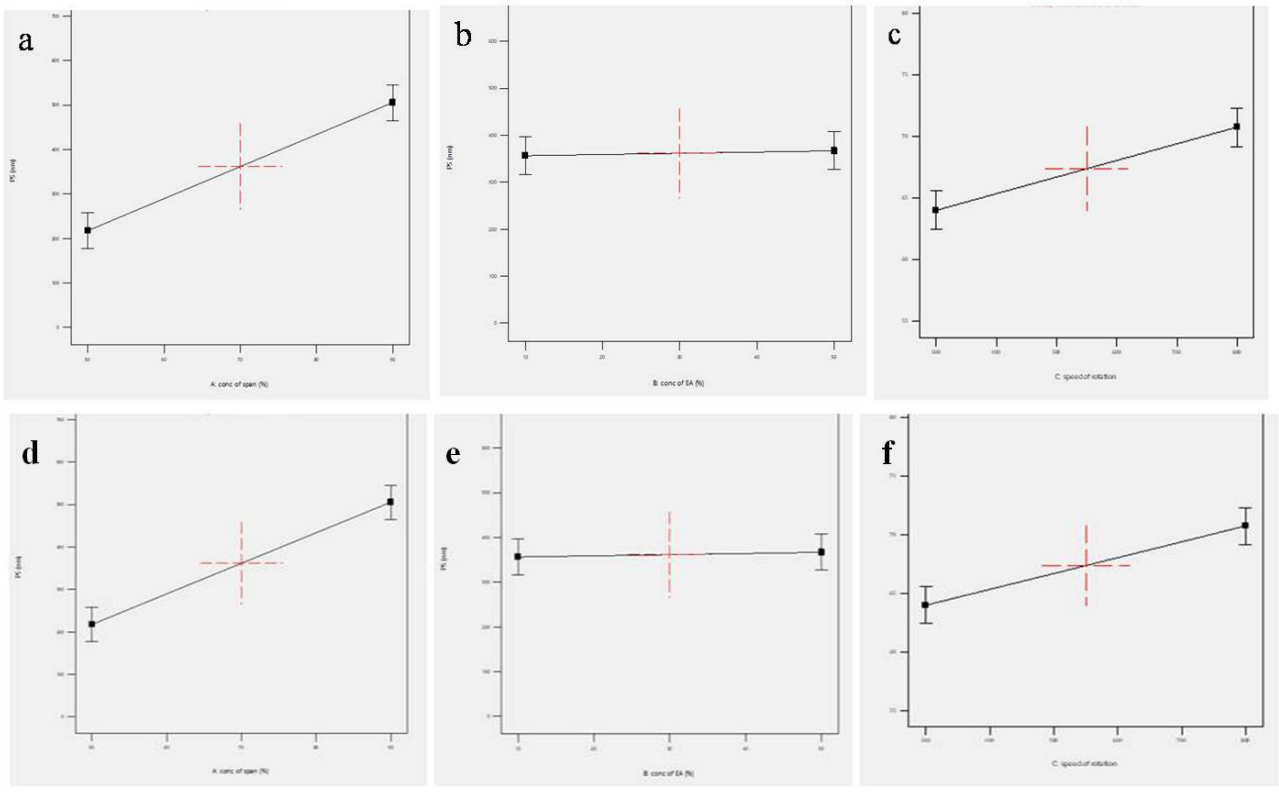

Figure 2. The effect of different factors (a) concentration of span 60, (b) concentration of EA and (c) speed of rotation on PS and the effect of factors (d) concentration of span 60, (e) concentration of EA and (f) speed of rotation on EE% of LPSp dispersion

2.6 Optimization of LPSp dispersions

Table 6 depicts the optimized formulation. The predicted value for PS and EE% were 372.463 nm and 75.949%, respectively. The desirable value of each factor and the contour plot for desirability is represented in Figure 3a and 3b respectively. The results that were observed through experiments were in accordance with the model prediction, thus establishing the credibility of the model. Further studies were done with the optimized LPSp formulation.

Table 6. Desireability of LPSp dispersion

No.	Concentration of span	Concentration of EA	Speed of rotation	PS (nm)	EE (%)	Desirability	
1	75.234	10.000	800.000	372.463	75.949	0.690	Selected

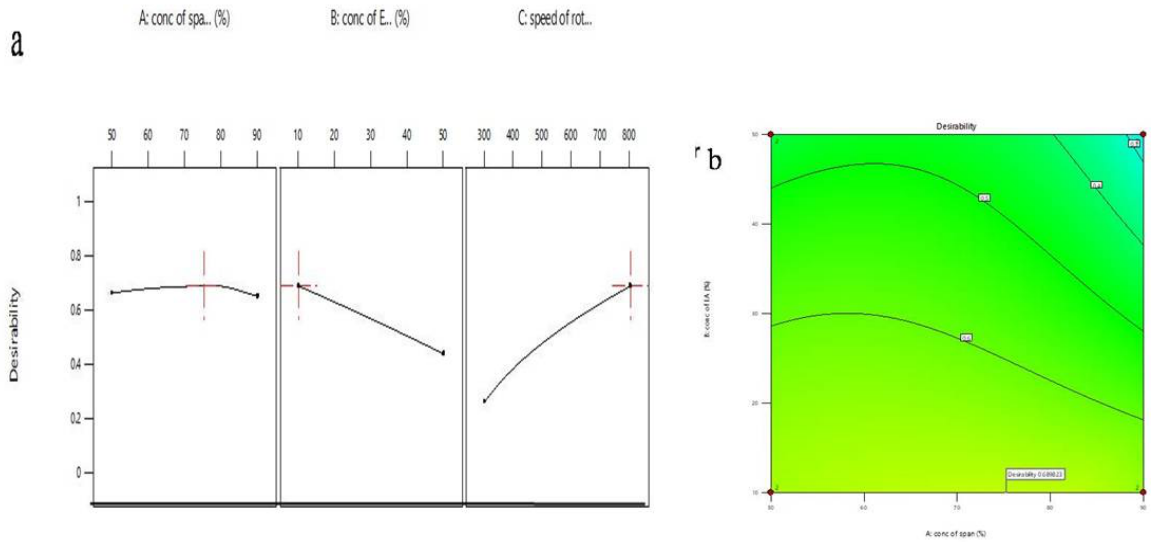

Figure 3. Graph (a) and Contour plot (b) for desirability of LPSp dispersions

2.7 Characterization of the optimized of LPSp dispersions

2.7.1 Measurement of PS, PDI, zeta potential and EE%

The PS of the optimized LPSp formula was found to be 320 nm (Figure 4a) with PDI value of 0.416. PDI values nearer to 0 indicate homogeneity and values approaching 1 indicates the presence of heterogeneous particles [19]. The optimized formula has a high negative zeta potential value of -44.8 mV (Figure 4b) specifying that the formula is stable and free from agglomeration. This may be due to the presence of ethanol that modifies the net charge of the system towards negative zeta potential and increases the steric stabilization [14]. The entrapment efficiency of the optimized formula was 72% which was in accordance with the value predicted by the software. This is due to the presence of saturated alkyl chain of Span 60 and its higher phase transition temperature (Tc = 53 ◦C) that resulted in decreased leakage of drug from the vesicle [18].

http://dx.doi.org/10.29228/jrp.187
J Res Pharm 2022; 26(4): 884-899

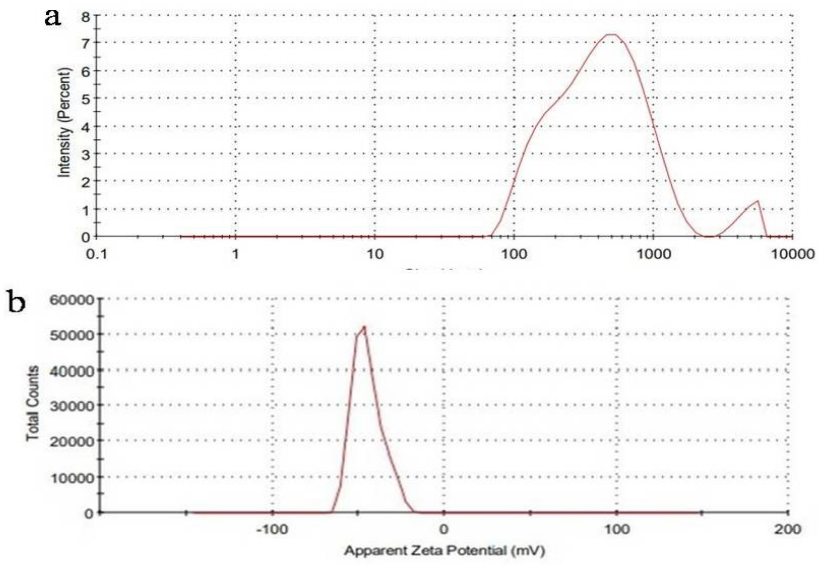

Figure 4. PS (a) and Zeta potential (b) of LPSp dispersions

2.7.2 Morphologic examination via Scanning Electron Microscopy (SEM)

The SEM image of LP spanlastic is depicted in Figure 5. The image shows almost spherical shaped particle with smooth surface.

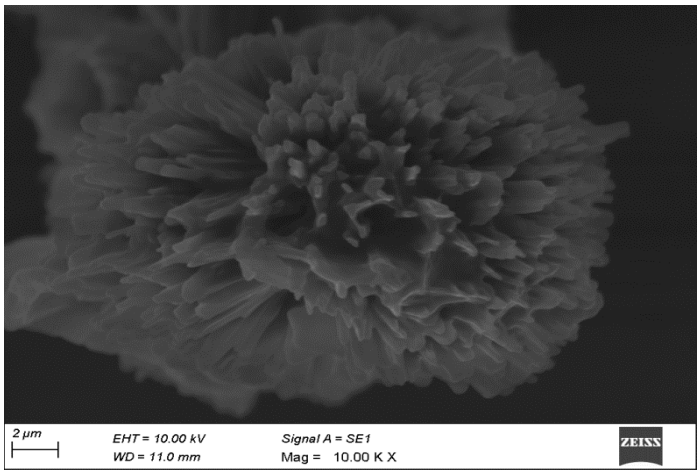

Figure 5. SEM micrograph of LPSp

2.8 Comparative evaluation of the optimized LPSp dispersion and conventional niosomes

The particle size, PDI and Zeta potential of LP loaded niosomes (LPNi) were 640 nm, 0.415 and -35.2 mV respectively. The particle size of LPNi was greater than the optimized LPSp formula. The EE% of LPNi were 46% lesser than that of optimized LPSp dispersion [18].

2.9 In- vitro drug release studies

The *in-vitro* drug release studies were carried for three formulations namely optimized LPSp, N1 and aqueous LP solution. The percentage drug release was calculated and graphically depicted in Figure 6. The aqueous LP drug solution released nearly 98.6% of the drug within 2h indicating rapid drug diffusion through the dialysis membrane. Furthermore, both the formulations LPSp and N1 showed sustained drug release over a period of 8h. The percentage of drug released initially over the first hour was 23.64% and 14.52% for N1 and LPSp respectively. Eventually, the percentage of drug release at the end of 8h was 85.08% and 96.39% for N1 and LPSp respectively. The increase in drug diffusion of LPSp when compared to LP loaded niosomes was

due to the enhanced flexibility of the LPSp vesicles. This might be due to the increase in elasticity of the vesicles which is attributed to the presence of edge activator [5].

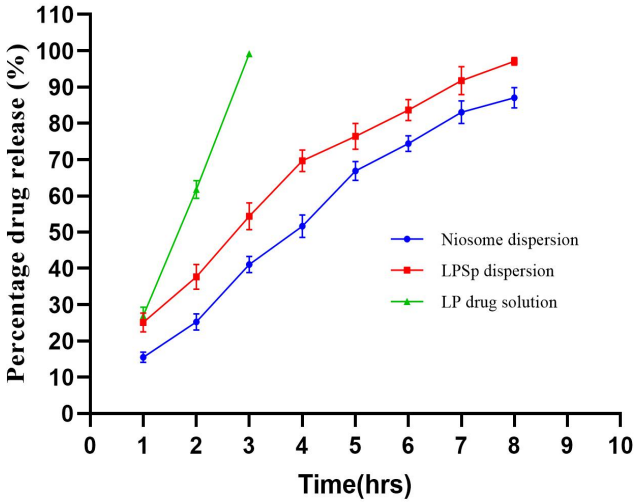

Figure 6. In- vitro drug release study of optimized LPSp, N1 and aqueous LP drug solution; (*n=3)

2.10 Formulation and evaluation of LPSp loaded bio-adhesive gel

Nano-Spanlastic Bio-adhesive gel (LPSpG) was formulated with the optimized formulation using Carbopol 940 (1%w/w).

2.10.1 Visual Inspection & pH measurement

The resulted gel was opaque, white in color with desired consistency, homogeneity, free from grittiness and pH value of 6.0. This value is in accordance with the pH of nasal mucosa (5.5-6.5). Therefore, the gel is suitable and non-irritant for nasal delivery.

2.10.2 Determination of drug content

The percentage drug content in LPSpG was 52.12% indicating that the formulation was not uniformly distributed in the gel structure.

2.10.3 Spreadability and extrudability

The spreadability of the gel is the property that indicates the ease with which the product can spread on the specified surface. The spreadability graph shows certain typical properties such as work of shear, firmness and stickiness. In the Figure 7a, the force appears to build until the cone probe reaches its maximum penetration depth. The firmness at the specified depth can be calculated using this peak force value. A harder sample has a greater area, which signifies the overall amount of force, also known as work of shear required to complete the shearing process. The work of shear and the firmness of the LPSp bio-adhesive gel are 333.485 g sec^{1} and 414.892 g respectively. The probe then withdraws from the sample, with any sticky properties indicated by a negative force reversal. Higher values of work of shear obtained for the optimum formulation was due to the use of mucoadhesive polymer (Carbopol 1%) which ensures prolonged adhesion to the mucosal surface [20].

The force required to push the gel out of the container is called Extrudability. It is vital for determining how easy it is to remove the gel out of the container. A compression-extrusion test involves applying force to the gel until it flows through an outlet. The product is squeezed until its structure is ruptured and at which point it extrudes from the container. The extrudability of LPSpG is 1494.448 g which is graphically depicted in Figure 7b.

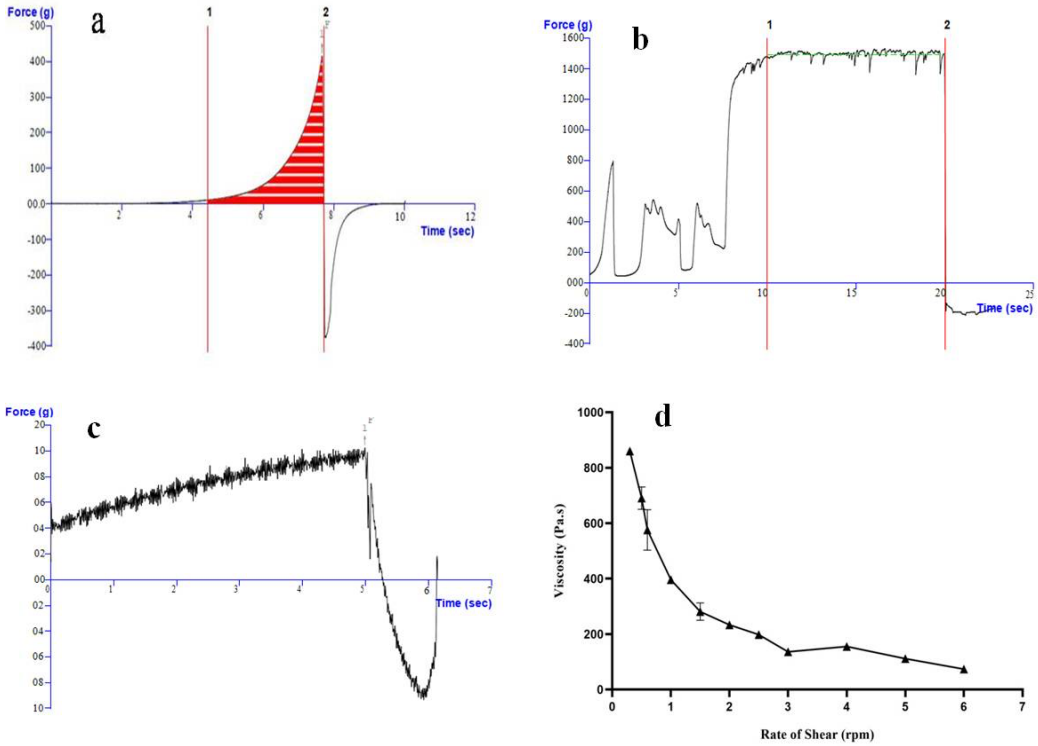

Figure 7. Spreadability (a), Bloom Strength (b), Extrudability (c) and Rheology (*n=3) (d) of LPSp bio-adhesive gel

2.10.4 Bloom strength

Bloom strength of a gel is the strength and stiffness of the gel also known as Bloom value. This value often reflects the average molecular weight of its constituents. The Bloom value of LPSp bio-adhesive gel is 10.286 g. It is graphically depicted in Figure 7c.

2.10.5 Rheology study of LPSp bio-adhesive gel

The viscosity of LPSpG decreased with increasing shear rate (Figure 7d). This indicates that the gel possessed a non-Newtonian (pseudo plastic) which explains that on increasing the shear rate there might be a rupture of internal structure of the gel [21].

2.10.6 Ex-vivo permeation studies

From the results, it was seen that the permeation rate LPSpG increased when compared to the permeation rate of LPNiG (Figure 8). Nearly 98% of LP permeated via the nasal mucosa by the end of 24 hrs. Although the percentage of LP permeated from the LPNiG by the end of 24 h was about 88%. The steady state flux of the LPSpG was 80.2µg/cm²/hr higher than that of LPNiG 75.4 µg/cm²/hr. This increased permeation may be by virtue of improved elasticity of the spanlastic vesicles formulated with edge activator, which aids in enhancing the elasticity of the vesicular membrane and therefore helps in augmented permeation.

The release kinetics of the LPSpG showed that Korsmeyer Peppas model with an r^2 value of 0.9943 was the best fitting model and the release exponent (n=0.492) revealed that transport mechanism of the drug through the gel followed non-fickian diffusion i.e., it follows both diffusion and erosion-controlled release [22].

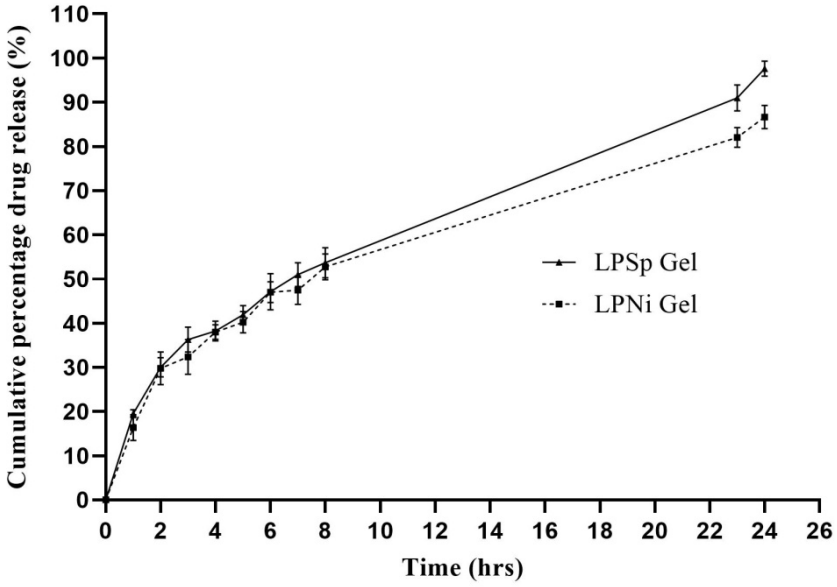

Figure 8. Ex-vivo permeation studies of LPSp and LPNi gels across goat nasal mucosa (*n=3)

2.10.7 Histopathological evaluation

The histopathological evaluation was done to comprehend the effects of formulation on the cell structure integrity. The study was carried out on both untreated and LPSp gel treated nasal mucosa (Figure 9). The epithelial cells were unscathed and well-conserved, with no evidence of necrosis or degeneration. The stroma portion of LPSpG treated nasal mucosa is seen with thick-walled dilated vessels. This dilation may be due to the pharmacological action of the anti-hypertensive drug Lisinopril dihydrate.

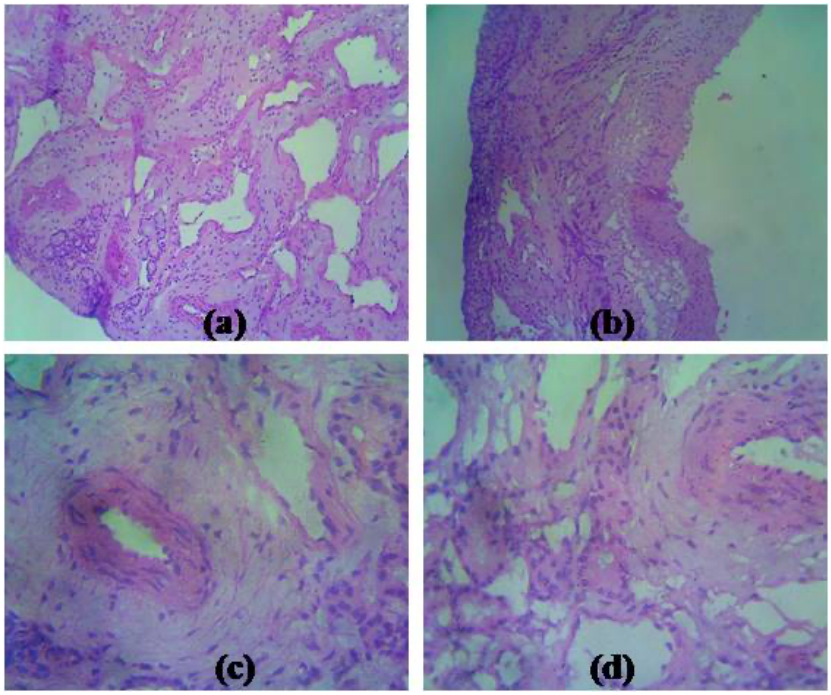

Figure 9. Histopathological evaluation of goat nasal mucosa (a) Normal tissue epithelium and sub-epithelium, (b) LPSp gel treated epithelium and sub-epithelium, (c) stroma portion of normal nasal mucosa and (d) stroma portion of LPSp gel treated nasal mucosa

3. CONCLUSION

In the present study, LP loaded nanospanlastic dispersions were prepared by ethanol injection method using span 60 and edge activator (tween 60 and tween 80). These nanospanlastics can improve the poor permeability of LP by squeezing through the narrow pores of biological membrane. The preliminary studies were carried out using span 60 as non-ionic surfactant and tween 60 and tween 80 as edge activators. From the pre-screening analysis, it was found that nanospanlastic formulation containing tween 80 as edge activator possessed the smaller size (92.67 nm) and higher entrapment efficiency (87.80 %); therefore, it was chosen for further optimization by 2^3 factorial design using Design Expert® software. A total of 8 runs were obtained to study the effect of concentration of Span 60, edge activator and speed of rotation on PS and EE% of LP nanospanlastics. The coefficient of determination (R2) and predicted/adjusted R2 of the chosen model were calculated for exploring its goodness of fit to the experimental results. Additionally, the significance level of the studied terms was investigated by the analysis of variance (ANOVA). This showed that the concentration of span 60 and speed of rotation had significant effect ($p<0.001$) on the PS and EE%. The formulation that has the highest desirability value was selected as the optimized formula. In the present study, the optimized formula was selected on the basis of minimum PS and maximum EE%. The optimized batch was subjected to surface morphological study which shows almost spherical shaped particles with smooth surface. The comparative in vitro release study was performed which indicates the drug enclosed in nanospanlastic dispersion shows higher diffusion compared to conventional niosome and aqueous LP solution. To overcome the drawbacks such as high first pass metabolism and decreased permeability, nasal route was preferred to deliver LP nanospanlastic. The optimized formula of LPSp was additionally formulated into a bio-adhesive gel using Carbopol (1%). The LPSp gels exhibited satisfactory results for pH, drug content, texture properties and rheology. The ex-vivo permeation study of LPSpG showed sustained and augmented permeation when compared to LPNiG.

This enhanced permeation of gel containing LP encapsulated into spanlastic vesicle can be considered to increase its bioavailability. The overall study concludes that, elastic vesicles made up of non- ionic surfactants can be propitious for increasing the permeation of drugs.

4. MATERIALS AND METHODS

Lisinopril dihydrate (LP) was obtained as a gift sample from Micro Labs Private Limited, Hosur, India. Sorbitan mono stearate (Span 60), Polyoxyethylene sorbitan monostearate (Tween 60), Polyoxyethylene sorbitan mono oleate (Tween 80) and Carbopol 940 were obtained from Loba Chemie Pvt. Ltd, Mumbai. Cellulose dialysis membranes (Dialysis membrane-70/pore size 2.4 nm, 12,000–14,000 Molecular weight cut-off) were obtained from HiMedia Laboratories Pvt. Ltd, Mumbai) and all other chemicals and solvents used were of analytical grade.

4.1 Fourier Transform-Infra Red Spectroscopy (FT-IR) studies

FT-IR studies were conducted to determine the chemical intermolecular interactions of the drug with the excipients. The spectral data were recorded by KBr pellet method using Fourier Transform Infrared Spectrophotometer (FT-IR 8400 Shimadzu 240V, Shimadzu Corporation). The samples were prepared as KBr pellets by compressing at 6 ton/nm^2. The wavelength ranges were selected between 400 and 4000cm^{-1}.

4.2 Pre-screening studies and Preparation of LPSp dispersions

Pre-screening studies were conducted to evaluate and choose different levels of formulation and operational variables that ameliorate the properties of LPSp formed from Span 60 with the addition of edge activator [23]. Ten different formulations (Table 2) were formulated using two different edge activators (Tween 80 and Tween 60) by ethanol injection technique. Briefly, the organic phase containing Span 60 dissolved in ethanol was sonicated for one minute. The preheated aqueous solution (at 60 ^oC) containing drug and the edge activator (Tween 60 or Tween 80) was injected into the organic phase at a rate of 1 ml/min, stirred at 500 rpm. The solution was continuously stirred for 30 minutes at 60^oC and 30 minutes on cold for complete evaporation of ethanol, ensuing formation of LPSp dispersions [24]. Ultrasonication was performed using ultrasonic bath sonicator (LUMC-3, LABMAN Scientific Instruments Pvt. Ltd, Chennai) with 40kHz frequency for 5 minutes, to obtain fine spanlastic dispersions and it was evaluated for PS and EE%. The edge activator that attained the best result was used for further studies.

4.3 Analysis of the 2^3 factorial design of LPSp dispersion

The selected Edge activator Tween 80, that had the smallest PS and highest EE% used in formulation of spanlastics was comprehended in the experimental design for further optimization. A 2^3 factorial design was used to develop and evaluate the correlation between independent variables and their responses using Design-Expert® (Version 7) software [25]. Concentrations of Span 60 (Factor 1), Concentration of EA (Factor 2) and Speed of rotation (Factor 3) were regarded as the independent variables. On the other hand, dependent variables (responses) were PS (Response 1), and EE% (Response 2). A total of eight runs were attained (Table 3). Desirability values were obtained to determine the optimum formula by analyzing the response surface of the acquired data (Table 6).

4.4 Characterization of LPSp dispersion

4.4.1 Measurement of PS, PDI, zeta potential

The average vesicle size and polydispersity index of prepared vesicles were evaluated using Malvern Zetasizer (Nano ZS90, Malvern instruments). The samples were placed in polystyrene cuvette at 25°C after dilution (1:100) with deionized water and the readings were measured at fixed angle. The PS and size distribution can be obtained [26, 27]. The zeta potential of the optimized vesicles was measured using Doppler electrophoresis integrated with the same equipment. The sample is placed in a cuvette and a dip cell containing the electrode was positioned into it. The measurement was carried out at 25 ± 0.5°C temperature after suitable dilution with deionized water [27, 28]. All the measurements were done in triplicate.

4.4.2 Determination of drug EE %

The unentrapped drug was segregated from drug-loaded vesicles by ultracentrifugation of the dispersions at a speed of 13,000 rpm for 1hr at 4°C [29]. The supernatant solution was collected and the amount of free drug released from the vesicles was determined by UV-visible spectrophotometer (UV 1650 PC, Shimadzu Corporation), after appropriate dilution at a wavelength of 207 nm. The percentage EE was measured in triplicate and calculated using the below equation

$$\text{EE (\%)} = \frac{\text{Initial amount of drug loaded (mg)- Unentrapped drug (mg)}}{\text{Amount of drug loaded (mg)}} \text{ X } 100$$

4.4.3 Morphologic examination via Scanning Electron Microscopy (SEM):

The morphologic examination of the optimized vesicles was done using Scanning Electron Microscope (Zeiss EVO® 18, Germany). The powder was coated with gold palladium before analysis and placed on aluminum stubs [30].

4.5 Comparative study of the optimized LPSp dispersion and conventional niosomes

A comparative study of LPSp dispersions were done with the corresponding LP loaded niosomes (LPNi). The conventional (LPNi) were formulated by the same technique used in the preparation of LPSp dispersions but replacing cholesterol in the place of EA in 50:50 ratio of surfactant and cholesterol respectively. The prepared LPNi was characterized for PS, PDI, zeta potential and EE% as previously described in section 4.4.1 and 4.4.2.

4.6 In-Vitro drug release studies:

The in-vitro release study of LPSp dispersion was carried out using open end cylinder. The dialysis membrane was first hydrated in the buffer solution at 25°C for 24 hours. The LPSp dispersions were placed over the dialysis membrane tied to the cylinder. The cylinder was immersed in 300 ml of phosphate buffer solution of pH 7.4. The receptor solution was stirred at 100 rpm maintained at 37 ± 0.5°C during the experiment. Samples (5 ml) were withdrawn and replaced with equal volume of fresh buffer at intervals of 1, 2, 3, 4, 5, 6, 7, and 8 and then after 24 h. Samples were analyzed in triplicate using UV- visible spectrophotometer at 207nm [25].

4.7 Formulation and evaluation of LPSp bio-adhesive gel

The optimized LPSp was formulated into a gel using Carbopol 940. The gel was prepared by slowly adding the calculated amount of Carbopol 940(1% w/v) while stirring to one third of the required amount with distilled water. To this Glycerin (1% w/v) was added as a humectant. The final volume was then made up to 100 ml with distilled water containing the optimized LPSp dispersions equivalent to 2.5 mg of LP/gm

of gel in 250 ml beaker and stirred at a high speed with mechanical stirrer, until a thin dispersion without lumps was obtained. Few drops of triethanolamine were added to form the gel. The prepared gels were stored overnight in the refrigerator [21].

4.7.1 Visual Inspection & pH measurement

The appearance of the gel and its physical properties including color, presence of lumps and homogeneity were inspected by visual inspection under black and white background. The pH of the gel was determined using digital pH meter (LI-120, ELICO). 1 gram of the formulated gel was taken in 10 ml volumetric flask and diluted to 10 ml with distilled water and its pH was measured [31].

4.7.2 Determination of drug content

1 gram of the formulated gel was dissolved in 100 ml of phosphate buffer pH 7.4 using mechanical shaker (KEMI orbital shaker) agitated at 50rpm for 2 hrs. Aliquots were withdrawn, filtered, diluted and its absorbance was measured at 207nm [32].

4.7.3 Spreadability and extrudability

Spreadability and extrudability of the formulated gel was determined using Texture Analyzer (TA.XT plus, Stable Microsystems). Spreadability was determined using spreadability rigs (perspex cones). The peak force and work of shear were measured. The extrudability of the formulated gel was measured using forward extrusion rig which measures the compression force required for a piston disc to extrude a product through a standard size outlet of 3mm diameter in the base of the sample container. The force required to extrude the gel was recorded.

4.7.4 Bloom strength

The bloom strength of the formulated gel was assessed using Texture Analyzer (TA.XT plus, Stable Microsystems) by measuring the mechanical resistance to stress. A cylindrical probe typically of 0.5-inch diameter is lowered into the gel system at a fixed speed. The gel strength is reported as the peak force reaching a chosen distance usually before permanent deformation [33].

4.7.5 Rheology study of LPSp gels

The viscosity of the formulated gel was determined using Brookfield's Viscometer. The freshly prepared gel was placed in the cup of the viscometer. The viscosity was determined using spindle size 64 at varying rpm, and the measurements were done in triplicate [32].

4.7.6 Ex-vivo permeation studies

The fresh goat nasal mucosa obtained from local slaughter house was used for permeation studies. A measured piece of the nasal mucosa was tied to one end of the open cylinder with the mucosal side facing the donor compartment. A calculated amount of LPSp bio-adhesive gel (1.9 g containing 2.5 mg of LP) was uniformly spread on the membrane and phosphate buffer of pH 7.4, was placed in the receptor compartment. The setup was maintained at 37±0.5°C. 5ml of samples were withdrawn at 30 min, 1, 2, 3, 4, 5, 6, 7, 8 and then 24 hrs and replaced with fresh medium in order to maintain sink condition. The samples were analyzed in triplicate by UV-visible spectrophotometer at 207 nm. The amount of drug permeated was calculated [34, 35]. The steady state flux J_{ss}, was calculated from the amount of LP permeated across 2.5 cm^2 of the nasal membrane over time using the following equation,

$$J_{ss} = \Delta Qt / (\Delta t \times S)$$

Where, Qt is the cumulative amount of Lisinopril permeated and S is the surface area of the membrane [35].

The permeation kinetics of LPSpG was analyzed by fitting the permeation data to different mathematical models like zero order, first order, Higuchi, Hixson-Crowell, Korsemeyer–Peppas diffusion models [36].

4.7.7 Histopathological evaluation

Histopathological studies were carried out to assess the viability of cells in the goat nasal mucosa after 24 h of permeation studies and compared with untreated mucosa. Initially, the membrane was refined and embedded with paraffin after fixing in 10% buffered formalin. Further paraffin sections (7µm) were taken, stained with haematoxylin and eosin and subjected for detailed microscopic examination [37].

4.8 Statistical Analysis

Design Expert® Software (Version 7.0) was used to analyze the data obtained by 2^3 factorial designs by conducting ANOVA to evaluate the influence of the selected factors on the PS, EE%.

Acknowledgements: The authors would like to thank PSG College of Pharmacy for providing all the required facilities for carrying out this work. This study was not supported financially

Author contributions: Concept – S.P., R.N.; Design – S.P.; Supervision – R.N; Resources –R.N., S.P.; Materials – R.N., S.P.; Data Collection and/or Processing – S.P.; Analysis and/or Interpretation –S.P., R.N; Literature Search –S.P.; Writing – S.P., R.N.; Critical Reviews – R.N., S.P.

Conflict of interest statement: The authors declared no conflict of interest in the manuscript.

REFERENCES

[1] Pandita A, Sharma P. Pharmacosomes: an emerging novel vesicular drug delivery system for poorly soluble synthetic and herbal drugs. ISRN Pharm. 2013; 3481-3486. [CrossRef]

[2] Mbah CC, Attama AA. Vesicular carriers as innovative nanodrug delivery formulations. In: Alexandru MG, (Eds). Organic Materials as Smart Nanocarriers for Drug Delivery. William Andrew Publishing, Romania, 2018, 519–559. [CrossRef]

[3] Jain S, Jain V, Mahajan SC. Lipid Based Vesicular Drug Delivery Systems. Adv Pharm. 2014, 2014(i):1–12. [CrossRef]

[4] Kakkar S, Kaur IP. Spanlastics-A novel nanovesicular carrier system for ocular delivery. Int J Pharm; 2011;413(1-2):202–10. [CrossRef]

[5] Jacob L, Anoop KR. A review on surfactants as edge activators in ultradeformable vesicles for enhanced skin delivery. Int J Pharma Bio Sci. 2013;4:337-334 [CrossRef]

[6] Lopez EO, Parmar M, Pendela VS, Terrell JM. Lisinopril. 2021;1–6. [CrossRef]

[7] Jagdale SC, Suryawanshi VM, Pandya S V, Kuchekar BS, Chabukswar AR. Development of press-coated, floating-pulsatile drug delivery of lisinopril. Sci Pharm. 2014;82(2):423–40. [CrossRef]

[8] Degenhard M, Gerallt W, Matthias B. Intranasal Drug Administration — An Attractive Delivery Route for Some Drugs In: Omboon V, Suleiman O, (Eds). Drug Discovery and Development - From Molecules to Medicine; 2015:229-320. [CrossRef]

[9] Sorrenti M, Catenacci L, Cruickshank DL, Caira MR. Lisinopril dihydrate: Single-crystal X-ray structure and physicochemical characterization of derived solid forms. J. Pharm. Sci. 2013; 102(10):3596-3603. [CrossRef]

[10] Mokale VJ, Patil HI, Patil AP, Shirude PR, Mokale VJ, Patil HI. Formulation and optimisation of famotidine proniosomes : an in vitro and ex vivo study Formulation and optimisation of famotidine proniosomes : an in vitro and ex vivo study. J Exp Nanosci 2015;11(2):97–110. [CrossRef]

[11] El-Sayed MM, Hussein AK, Sarhan HA, Mansour HF. Flurbiprofen-loaded niosomes-in-gel system improves the ocular bioavailability of flurbiprofen in the aqueous humor. Drug Dev Ind Pharm. 2017; 43(6): 902-910. [CrossRef]

[12] Khoee S, Yaghoobian M. Niosomes: A novel approach in modern drug delivery systems. In: Ecaterina A, Alexandru MG, (Eds). Nanostructures for drug delivery. 2017: 207-237. [CrossRef]

[13] Junyaprasert VB, Singhsa P, Suksiriworapong J. Physicochemical properties and skin permeation of Span 60 / Tween 60 niosomes of ellagic acid. Int J Pharm. 2012;423(2):303–311. [CrossRef]

[14] Tayel SA, El-Nabarawi MA, Tadros MI, Abd-Elsalam WH. Duodenum-triggered delivery of pravastatin sodium via enteric surface-coated nanovesicular spanlastic dispersions: development, characterization and pharmacokinetic assessments. International journal of pharmaceutics. 2015;10;483(1-2):77-88. [CrossRef]

[15] Kaur IP, Rana C, Singh M, Bhushan S, Singh H, Kakkar S. Development and evaluation of novel surfactant-based elastic vesicular system for ocular delivery of fluconazole. J Ocul Pharmacol Ther. 2012; 28(5):484-96. [CrossRef]

[16] Chauhan B, Gupta R. Application of statistical experimental design for optimization of alkaline protease production from Bacillus sp. RGR-14. Process Biochem .2004; 39(12):2115-2122. [CrossRef]

[17] Ruckmani K, Sankar V. Formulation and optimization of Zidovudine niosomes. AAPS PharmSciTech. 2010 ;11(3):1119-27. [CrossRef]

[18] Mazyed EA, Helal DA, Elkhoudary MM, Abd Elhameed AG, Yasser M. Formulation and optimization of nanospanlastics for improving the bioavailability of green tea epigallocatechin gallate. Pharmaceuticals. 2021 ;14(1):1–30. [CrossRef]

[19] Zeisig R, Shimada K, Hirota S, Arndt D. Effect of sterical stabilization on macrophage uptake in vitro and on thickness of the fixed aqueous layer of liposomes made from alkylphosphocholines. Biochimica et Biophysica Acta (BBA)-Biomembranes.1996; 1285(2):237-45. [CrossRef]

[20] Grina, Donatas. Technology and analysıs of semısolıd preparatıons wıth tolnaftate. 2011. [CrossRef]

[21] Abhaihaidelmonem R, Nabarawi M El, Attia A. Development of novel bioadhesive granisetron hydrochloride spanlastic gel and insert for brain targeting and study their effects on rats. Drug Deliv. 2018;25(1):70–77. [CrossRef]

[22] Dash S, Murthy PN, Nath L, Chowdhury P. Kinetic modeling on drug release from controlled drug delivery systems. Acta Pol Pharm - Drug Res. 2010;67(3):217–23. [CrossRef]

[23] Badria F, Mazyed E. Formulation of nanospanlastics as a promising approach for improving the topical delivery of a natural leukotriene inhibitor (3-acetyl-11-keto-β-boswellic acid): Statistical optimization, in vitro characterization, and ex vivo permeation study. Drug Des Devel Ther. 2020;14:3697–3721. [CrossRef]

[24] Liu Y, Wang Y, Yang J, Zhang H, Gan L. Cationized hyaluronic acid coated spanlastics for cyclosporine A ocular delivery : Prolonged ocular retention , enhanced corneal permeation and improved tear production. Int J Pharm. 2019;565:133–42. [CrossRef]

[25] Farghaly DA, Aboelwafa AA, Hamza MY, Mohamed MI. Topical Delivery of Fenoprofen Calcium via Elastic Nano-vesicular Spanlastics: Optimization Using Experimental Design and In Vivo Evaluation. AAPS PharmSciTech. 2017;18(8):2898-2909. [CrossRef]

[26] Zeng W, Li Q, Wan T, Liu C, Pan W, Wu Z. Hyaluronic acid-coated niosomes facilitate tacrolimus ocular delivery: Mucoadhesion, precorneal retention, aqueous humor pharmacokinetics, and transcorneal permeability. Colloids Surfaces B Biointerfaces. 2016;141:28–35. [CrossRef]

[27] Zetasızer nano series Performance, Sımplıcıty, Versatılıty. [CrossRef]

[28] Sohrabi S, Haeri A, Mahboubi A, Mortazavi A, Dadashzadeh S. Chitosan gel-embedded moxifloxacin niosomes: An efficient antimicrobial hybrid system for burn infection. Int J Biol Macromol. 2016;85:625–633. [CrossRef]

[29] Abdelbari MA, El-Mancy SS, Elshafeey AH, Abdelbary AA. Implementing spanlastics for improving the ocular delivery of clotrimazole: In vitro characterization, ex vivo permeability, microbiological assessment and in vivo safety study. Int J Nanomedicine. 2021;16:6249–61. [CrossRef]

[30] Demirbolat GM, Aktas E, Pelin G, Omer C, Ozge E. New Approach to Formulate Methotrexate-Loaded Niosomes : In Vitro Characterization and Cellular Effectiveness. J Pharm Innov. 2021:1-16. [CrossRef]

[31] Jana S, Manna S, Kumar A, Kumar K. Carbopol gel containing chitosan-egg albumin nanoparticles for transdermal aceclofenac delivery. Colloids Surf. B. 2014;114:36–44. [CrossRef]

[32] Patel RP, Patel HH, Baria AH. Formulation and Evaluation of Carbopol Gel Containing Liposomes of Ketoconazole. (Part-II). Int. J. Drug Deliv. Technol. 2009;1(2):42-45. [CrossRef]

[33] Sareen R, Kumar S, Gupta GD. Meloxicam Carbopol-Based Gels: Characterization and Evaluation. Curr. Drug Deliv. 2011;8(4):407–415. [CrossRef]

[34] Basu S, Maity S. Preparation and characterisation of mucoadhesive nasal gel of venlafaxine hydrochloride for treatment of anxiety disorders. Indian J. Pharm. Sci. 2012; 74(5):428. [CrossRef]

[35] Barakat NS. Evaluation of glycofurol-based gel as a new vehicle for topical application of naproxen. AAPS Pharmscitech. 2010;11(3):1138-1146. [CrossRef]

[36] De PK, Ghatak S. Formulation Optimization, Permeation Kinetic and Release Mechanism Study of In-Situ Nasal Gel Containing Ondansetron. Saudi J Med Pharm Sci. 2020; 6(1):91-101. [CrossRef]

[37] Tzeyung AS, Md S, Bhattamisra SK, Madheswaran T, Alhakamy NA, Aldawsari HM, Radhakrishnan AK. Fabrication, optimization, and evaluation of rotigotine-loaded chitosan nanoparticles for nose-to-brain delivery. Pharmaceutics. 2019;11(1):26. [CrossRef]